Robotics and Computer-Integrated Manufacturing 28 (2012) 517–529

Contents lists available at SciVerse ScienceDirect

Robotics and Computer-Integrated Manufacturing

journal homepage: www.elsevier.com/locate/rcim

Index based optimal anatomy of a metamorphic manipulator for a given task

Charalampos Valsamos [a,*], Vassilis Moulianitis [b], Nikos Aspragathos [a]

[a] Mechanical and Aeronautics Engineering Department, University of Patras, 26500 Rio, Achaia, Greece
[b] Department of Product and Systems Design Engineering, University of Aegean, 84100 Ermoupolis, Syros, Greece

ARTICLE INFO

Article history:
Received 8 October 2010
Received in revised form
14 October 2011
Accepted 20 November 2011
Available online 2 February 2012

Keywords:
Metamorphic manipulators
Manipulability index
Manipulator velocity ratio
Optimal anatomy
Product of exponentials formula

ABSTRACT

This paper introduces an approach for the determination of the best anatomy of a metamorphic manipulator for a given task at a given location. The location of the task is determined by maximizing the performance of a current industrial fixed anatomy robot. Two types of tasks are considered: a point to point task and a path following task, where in the first case the approximated minimum of the manipulability index is formed along the task points and in the second case the approximated minimum of the manipulator velocity ratio is formed along the line segments. These indexes are maximized in order to determine the best anatomy for the task. The proposed approach is tested and the results show that the determined best anatomy for each type of task acquired higher performance than the respective one achieved by the fixed anatomy manipulator.

1. Introduction

A fixed anatomy robot can perform different tasks by changing its programming, albeit each industrial robot has a specific anatomy and capabilities supporting a limited type of applications. Metamorphic (reconfigurable) robots have been proposed in the relevant literature for their innate ability to alter their anatomy in order to meet the demands of different tasks. During the design phase of metamorphic workcells a key issue to be addressed is the determination of the best anatomy for the given task. Currently, this procedure usually follows well established practices for the current fixed anatomy manipulators, adapted to the characteristics of metamorphic manipulators.

The relevant literature for open chain fixed anatomy manipulator workcell design is quite rich and abundant with different methods and indices and is presented in the following section together with the contribution of the present work. In the third section the structuring of a metamorphic manipulator using pseudo joints is presented. Then the methodology for deriving the optimal anatomy of the metamorphic manipulator is presented. The case study problems are presented and formulated. The simulation algorithms used are also described. Finally, the results of the test cases for the selected tasks and robotic systems are presented and discussed.

2. State-of-the-art survey

A method based on Genetic Algorithms was presented to determine the optimal location of a path to be followed by a fixed manipulator's end-effector, where the robot presents the higher velocity performance [1]. The objective function used in this method was a task based measure for the velocity efficiency (approximation of the minimum of the Manipulator Velocity Ratio) of a robot for a path following task presented in [2]. In [3], the overall manipulability measure and the relative stroke of workspace were proposed as design criteria for optimal kinematics design of a 6 degree of freedom serial robot manipulator. A kinematics performance index based on the rate of change of a standard isotropy condition for robot kinematic design optimization and the determination of its best configuration was presented and applied to the optimal kinematic design and best posture determination of a redundant manipulator in [4]. In [5], a combined performance index resulting from an aggregation of the manipulability measure and the condition number of the Jacobean was introduced. In this work, optimization was performed under two objectives, the maximization of the workspace volume of the robot and the maximization of the introduced index.

The determination of the best anatomy of a modular manipulator for a given task has also been under research, as reconfigurable robots gained much interest. In [6], a methodology was presented for the optimization of the anatomy of a reconfigurable robotic workcell, where the objective function was formulated considering robot performance for a particular task. In [7], a method for the optimal design of a modular robot satisfying particular task requirements based on the minimal degrees of

* Corresponding author. Tel.: +302610997212; fax: +302610996142.
E-mail addresses: balsamos@mech.upatras.gr (C. Valsamos), moulianitis@syros.aegean.gr (V. Moulianitis), asprag@mech.upatras.gr (N. Aspragathos).

0736-5845/$ - see front matter © 2011 Elsevier Ltd. All rights reserved.
doi:10.1016/j.rcim.2011.11.006

freedom approach was proposed using the Assembly Incidence Matrix (AIM). The objective function was defined as the weighted sum of the score of different types of modules in the AIM, while task related kinematic measures were used as design constraints. An approach using a configuration engine capable of generating and designing different symmetric parallel and serial manipulator architectures for a given task was presented in [8,9].

In the above presented methods regarding the design of modular robotic workcells the following can be noticed. When a new task should be performed, a new anatomy is determined as the optimal one for this task. During the anatomy transition the modular manipulator is disassembled at least partially and reassembled to the new anatomy. Such a procedure requires considerable down times albeit being faster and less costly than replacing the manipulator with a new one, more suited to the task. All emerging modular anatomies comply with the current design practice of fixed anatomy robots in use. Lastly, although advantages of modular reconfigurable robots have been discussed to a great degree from a qualitative point of view a quantitative performance comparison between them and fixed anatomy robots has not been conducted to support these advantages.

The contribution of this work is threefold. Firstly, previous work on the optimal task location for fixed anatomy manipulators is extended and modified so as to develop an approach leading to the determination of the optimal anatomy for a metamorphic manipulator for a given task. The main aim of this approach is the determination of the anatomy that best adapts to the task, taken into account the suitable performance measure of the manipulator for the given task and considering the angles of the pseudo joints as the optimization parameters. Secondly, metamorphic robots and the pseudo joint concept is presented as a means to structure them and transform them from the current anatomy to the one best suited for the given task in very short time (towards zero downtime). Thirdly, since the tasks to be undertaken by the metamorphic system are considered to be optimally placed in the fixed anatomy robot's workspace the comparison of their performance for similar tasks is allowed and an insight on whether a metamorphic robot is more advantageous than a fixed anatomy one can be given.

3. The metamorphic manipulator

In this work, metamorphic manipulators are proposed as a class of modular reconfigurable robots that allow changes in their anatomy to take place without the need for dismantling and reassembling their anatomy. As such, this particular class of manipulators is ideal for usage in SME's where fully customizable products are produced in small batches, depending on the customer's needs, therefore a wide variety of different tasks to be undertaken by a robot are presented. Due to their dedicated design addressing specific ranges of tasks, fixed anatomy robots are not considered practical since in order to execute different tasks they would have to be reprogrammed from scratch, while the tasks will have to be designed so as for the robot to achieve the best possible performance. Modular reconfigurable robots can undertake far more tasks by allowing the disassembling and reassembling of their anatomy to a different one [6,10,11]. Such a feature requires extensive down times, albeit being a faster and more economic solution than the replacement of an existing fixed anatomy robot with a new one. Metamorphic manipulators are proposed in this work as a solution that can address the disadvantages of these designs. An initial anatomy can be structured that can be altered without dismantling in a rapid and effortless fashion. By matching a different anatomy to the desired task the metamorphic manipulator can undertake a wide variety of tasks.

3.1. Pseudo joints

The concept of pseudo joints was presented as a means to facilitate the rapid anatomical reconfiguration of an articulated manipulator [12]. Practically, they are passive connectors that can be used to manually change the anatomical parameters of the manipulator. Their application allows the insertion of desired rotational axes between the various modules composing a metamorphic articulated manipulator. These allow the rapid alteration of the manipulator's anatomy as they allow the changing of the relative position and orientation between consecutive joints.

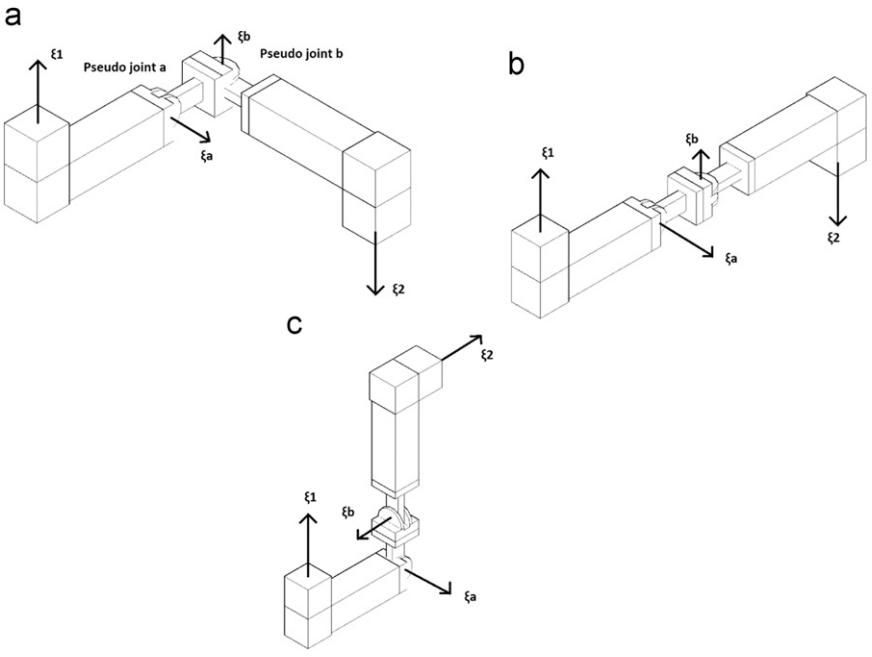

Fig. 1. Reconfiguration of the mechanism using pseudo joints.

Fig. 1 illustrates the rapid manual metamorphosis of a 2 d.o.f. mechanism whose joint twist are denoted (ξ_1,ξ_2) via the rotation of its components about the inserted twists ξ_a and ξ_b of two pseudo joints **a** and **b**.

The mechanism consists of 2 active rotational joints, two rigid links and two pseudo joints, which will facilitate its rapid reconfiguration. In Fig. 1(a), the mechanism is shown at its reference anatomy, where all pseudo joints in the robot's lattice are considered to be at their starting configuration where their angles are set to 0°. The designer can specify a twist corresponding to the placement of the pseudo joint at the reference anatomy of the manipulator. The orientation of the twist, along with the choice of the reference configuration of the pseudo joint, allows the formulation of the exponential matrices that specify the induced rigid transformation from its displacement. The positive angle of rotation is considered to be that of following the right hand rule for the specified twist orientation. Therefore in Fig. 1(a) the pseudo joint angles are $\theta_a=\theta_b=0^\circ$.

The reconfiguration to the desired anatomy is achieved via the subsequent rotation required about each of the two inserted twists ξ_a and ξ_b (Fig. 1(b) and (c)). The reconfiguration is conducted by first rotating pseudo joint **b** by 90°, which results in the anatomy depicted in Fig. 1(b), where the pseudo joint angles are $\theta_a=0^\circ$ and $\theta_b=90^\circ$. Next pseudo joint **a** is rotated to $\theta_a=90^\circ$ so the mechanism is transformed to the desired anatomy (Fig. 1(c)) where the pseudo joint angles are $\theta_a=\theta_b=90^\circ$.

Pseudo joints also allow the operator to achieve anatomies of a metamorphic manipulator that are not currently favored in robotic design, i.e. in D–H representation presenting link twists different to the standard 0° or 90° of current robotic systems or in screw representation consecutive joint twists being either parallel or perpendicular. The link twist is the angle between two successive joint axes (joint twists) if these are projected on a plane whose normal coincides with the mutual perpendicular to the successive joint twists. Additionally, the placement of pseudo joints in the robot's lattice at specific orientations allows the formulation of metamorphic manipulators whose emerging anatomies kinematics can be solved [13]. According to Gao [14] a 6 d.o.f. manipulator allows the derivation of analytical solution to its kinematics if at least one pair of the first three consecutive joint twists is either parallel or intersects at a point.

3.2. The case study manipulator

In Fig. 2 the case study 6 d.o.f. metamorphic manipulator is shown in its reference anatomy and configuration.

The reference anatomy is defined as the one where all the pseudo joint angles are considered to be set equal to 0° and this particular anatomy is that of a 6 d.o.f. PUMA type articulated (Fig. 2). It is structured using three active rotational joints (ξ_1,ξ_2,ξ_3), six pseudo joints (ξ_a,ξ_b,ξ_c,ξ_d,ξ_e,ξ_f), rigid links and a spherical joint (ξ_4,ξ_5,ξ_6) consisting of three active rotational joints whose axes intersect at one point. This particular arrangement is consistent to most 6 d.o.f. manipulators allowing the extraction of an analytical solution to the inverse kinematics [13,14], since the presented set-up of the manipulator components is such that the twists of the second and third active joints will be either parallel or will intersect at a point. The reference configuration is chosen to be such that all the active joint angles are set to 0° and the orientation of the tool frame **{T}** (also depicted) is identical to that of the base coordinate system of the robot **{B}**. Fig. 2 also depicts the main lengths of the manipulator links.

The reconfiguration of the manipulator's anatomy to a new one is achieved by changing the pseudo joint angle settings. For each new anatomy the pseudo joints are considered rigid and set to the desired angle, which is changed only during the metamorphosis from one anatomy to the next one. The particular set-up of the robots structure, i.e. the sequence and orientation of pseudo joints, links and active joints were chosen so that the manipulator will be able to achieve a wide range of anatomies, which would include both anatomies that are "in line" with current practice in manipulator design and anatomies that are not favored in current practice. The main advantage of this set-up is the ability to easily match an anatomy to a given task in order to achieve higher performance.

As stated the considered anatomical parameters of the manipulator are the setting angles of the pseudo joints. These settings also determine the relative link twists (according to the D–H representation), as shown in Table 1 for the reference configuration and anatomy. The link twists of the spherical wrist are considered to be non-changeable.

In order to structure the kinematics of the manipulator, the orientation of the active joint twists, given by a unit vector $\boldsymbol{\omega}_i$

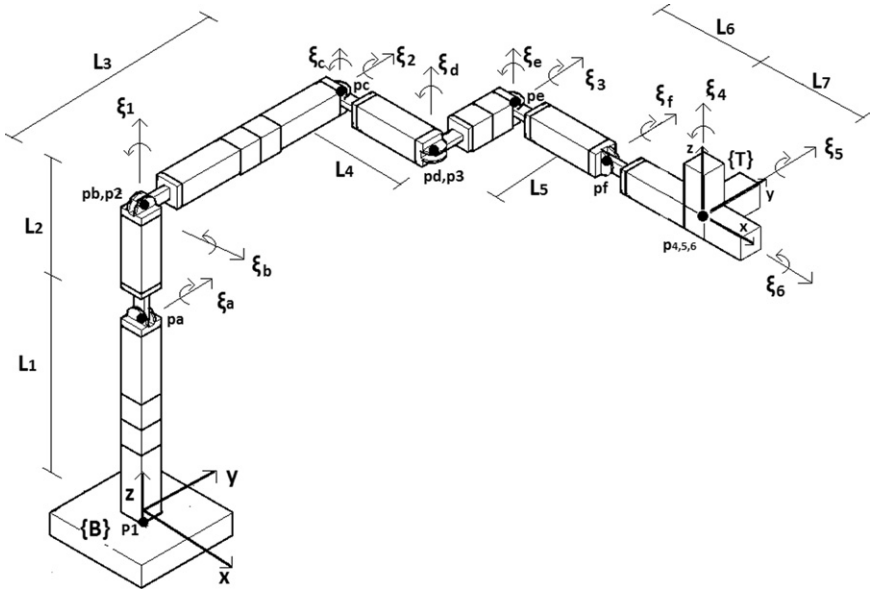

Fig. 2. Case study metamorphic manipulator.

$i=1,\ldots 6$ and the location of a point on each twist (both illustrated in Fig. 2) have to be determined. Of particular interest is the derivation of the location of the points on the active joint twists and their orientation, as a function of the pseudo joint angles. Table 2 depicts the equations leading to the derivation of the orientation of the active joint twists relative to **{B}** and the equations for deriving the location of a point on each active joint twist relative to **{B}** as a function of the pseudo joint twists. Using the data from these tables for each anatomy depicted by the pseudo joint angles ($\boldsymbol{\theta}_p=[\theta_a, \theta_b, \theta_c, \theta_d, \theta_e, \theta_f,]$), and considering the manipulator at its reference configuration ($\boldsymbol{\theta}=0$), it is possible to structure the manipulator kinematics for each emerging anatomy.

The manipulator's lengths are considered to be the following: $L_1=1.5$ m, $L_2=0.7$ m, $L_3=1.2$ m, $L_4=0.4$ m, $L_5=0.7$ m, $L_6=0.5$ m and $L_7=0.5$ m.

4. Determination of the best anatomy for a given task placed at a specific location

In this section, the approach for the determination of the best anatomy for a given task placed at a specific location is presented. The task is placed at an optimal location inside the workspace of a fixed anatomy manipulator, which is then replaced by a metamorphic one, whose best anatomy in terms of manipulability should be determined. Fig. 3 presents the procedure of the proposed method.

Such a set-up can help provide an insight on the level of performance achieved by the two systems, and provide a means for comparison. Although the practical advantages of metamorphic robots as opposed to fixed anatomy ones are discussed extensively and qualitative comparisons between the two have already been published [6], quantitative results comparing the performance of these systems while performing actual tasks were not presented in the relevant literature. In order to facilitate this comparison, which is one of the aims of this work, some key parameters need to be defined.

Table 1
Link twists in the reference anatomy.

Joint pair	ξ_1 and ξ_2	ξ_2 and ξ_3	ξ_3 and ξ_4
Link twist angle	$\alpha_1(\theta_a,\theta_b)=90^\circ$	$\alpha_2(\theta_c,\theta_d)=0^\circ$	$\alpha_3(\theta_e,\theta_f)=90^\circ$

4.1. Key parameters

The two types of manipulators present identical modules, structure and anatomy for at least one anatomical configuration achieved by the metamorphic system in order to (a) provide a starting point for the determination of the performance and (b) to allow the comparison of the two systems under similar conditions.

Since each task is optimally located so that the performance of the fixed anatomy system is the best possible, then by substituting the fixed anatomy robot with the metamorphic one and determining the optimal anatomy for the given task, a comparison on the performance of metamorphic manipulators against current fixed anatomy robots can be performed.

4.2. Optimal location of the tasks in the fixed manipulator's workspace

Two of the most commonly met robotic tasks in the manufacturing industry are point visiting tasks and path following tasks. For the purposes of this work, a task of both types is chosen to be performed by the two systems. As a first step, the two tasks are to be placed in an optimal location in the fixed anatomy manipulator's workspace.

4.2.1. Point visiting task

Spot welding or pick and place are the most common point to point industrial applications for a manipulator. For these tasks, a set of points on an object are defined and the manipulator end effector has to reach them. The object should be placed at the optimal location in the manipulator's workspace considering the robot performance [1,2].

Table 2
Twist orientation and point location of the active joint twists as a function of pseudo joint angles.

Twist	$\boldsymbol{\omega}_i$	Point
ξ_1	$\begin{bmatrix}0\\0\\1\end{bmatrix}$	$\begin{bmatrix}0\\0\\0\\1\end{bmatrix}$
ξ_2	$e^{\hat{\omega}_a\theta_a}e^{\hat{\omega}_b\theta_b}\begin{bmatrix}0\\1\\0\end{bmatrix}$	$e^{\hat{\xi}_a\theta_a}e^{\hat{\xi}_b\theta_b}\begin{bmatrix}0\\0\\L_1+L_2\\1\end{bmatrix}$
ξ_3	$e^{\hat{\omega}_a\theta_a}e^{\hat{\omega}_b\theta_b}e^{\hat{\omega}_c\theta_c}e^{\hat{\omega}_d\theta_d}\begin{bmatrix}0\\1\\0\end{bmatrix}$	$e^{\hat{\xi}_a\theta_a}e^{\hat{\xi}_b\theta_b}e^{\hat{\xi}_c\theta_c}e^{\hat{\xi}_d\theta_d}\begin{bmatrix}L_4\\L_3\\L_1+L_2\\1\end{bmatrix}$
ξ_4	$e^{\hat{\omega}_a\theta_a}e^{\hat{\omega}_b\theta_b}e^{\hat{\omega}_c\theta_c}e^{\hat{\omega}_d\theta_d}e^{\hat{\omega}_e\theta_e}e^{\hat{\omega}_f\theta_f}\begin{bmatrix}0\\0\\1\end{bmatrix}$	$e^{\hat{\xi}_a\theta_a}e^{\hat{\xi}_b\theta_b}e^{\hat{\xi}_c\theta_c}e^{\hat{\xi}_d\theta_d}e^{\hat{\xi}_e\theta_e}e^{\hat{\xi}_f\theta_f}\begin{bmatrix}L_4+L_6+L_7\\L_3+L_5\\L_1+L_2\\1\end{bmatrix}$
ξ_5	$e^{\hat{\omega}_a\theta_a}e^{\hat{\omega}_b\theta_b}e^{\hat{\omega}_c\theta_c}e^{\hat{\omega}_d\theta_d}e^{\hat{\omega}_e\theta_e}e^{\hat{\omega}_f\theta_f}\begin{bmatrix}0\\1\\0\end{bmatrix}$	$e^{\hat{\xi}_a\theta_a}e^{\hat{\xi}_b\theta_b}e^{\hat{\xi}_c\theta_c}e^{\hat{\xi}_d\theta_d}e^{\hat{\xi}_e\theta_e}e^{\hat{\xi}_f\theta_f}\begin{bmatrix}L_4+L_6+L_7\\L_3+L_5\\L_1+L_2\\1\end{bmatrix}$
ξ_6	$e^{\hat{\omega}_a\theta_a}e^{\hat{\omega}_b\theta_b}e^{\hat{\omega}_c\theta_c}e^{\hat{\omega}_d\theta_d}e^{\hat{\omega}_e\theta_e}e^{\hat{\omega}_f\theta_f}\begin{bmatrix}1\\0\\0\end{bmatrix}$	$e^{\hat{\xi}_a\theta_a}e^{\hat{\xi}_b\theta_b}e^{\hat{\xi}_c\theta_c}e^{\hat{\xi}_d\theta_d}e^{\hat{\xi}_e\theta_e}e^{\hat{\xi}_f\theta_f}\begin{bmatrix}L_4+L_6+L_7\\L_3+L_5\\L_1+L_2\\1\end{bmatrix}$

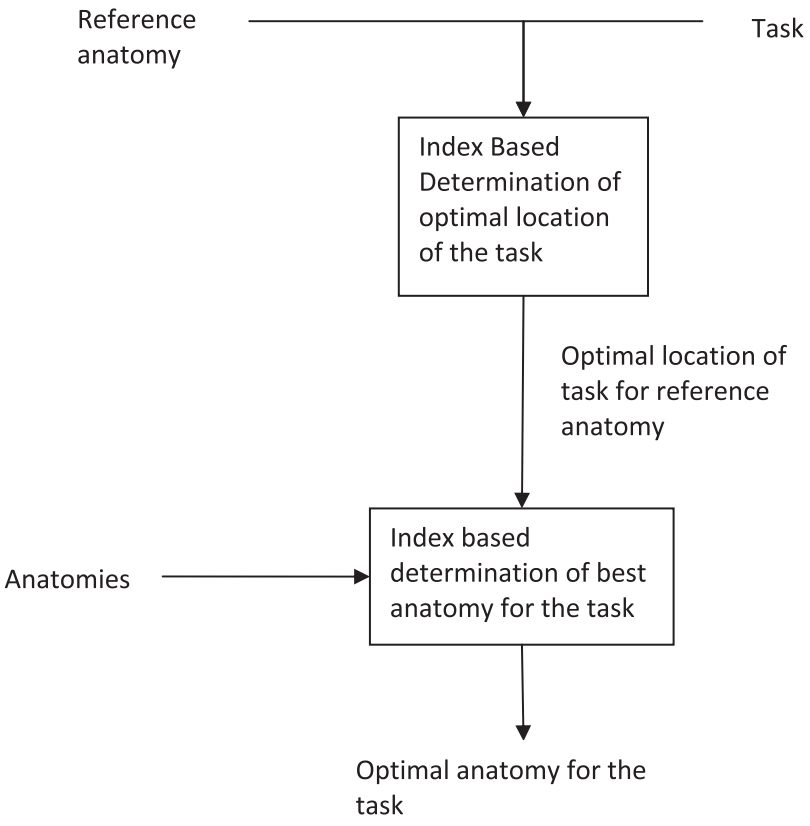

Fig. 3. Procedure of the presented method.

A task based performance index for the performance of manipulators in point to point tasks is formulated based on the well known Yoshikawa's manipulability index **w** [2]. The manipulability index is a quantified indication of the ability of the robot to move its end effector with large or small speeds in certain directions. The manipulability measure is also a quantitative measure of distance of the current (local) configuration of a manipulator from a singular one. The higher its value the farther from a possible singularity the manipulator lies, and therefore large values of the manipulability index are sought.

The manipulator is required to be able to reach k points in its workspace, which must be placed in such a location where it exerts the best possible manipulability performance. It is considered that the task points positions and orientations relative to a local coordinate system **{S}** located at one of the points to be visited are known and given by

$$ {}^{S}T_i = \begin{bmatrix} & \mathbf{R}_i & & \mathbf{q}_i \\ 0 & 0 & 0 & 1 \end{bmatrix}, \quad i = 2\ldots k \tag{1} $$

where $\mathbf{R}_i$ is the 3×3 matrix representing the orientation of the ith point coordinate system relative to **{S}** and $\mathbf{q}_i$ is the 3×1 vector representing the location of the ith point relative to **{S}**.

The tool frame **{T}** has to reach each of the k points whose orientation and position relative to **{B}** should be determined by the optimization algorithm. Considering this definition, the optimal placement of a task points cluster, is transformed to that of the optimal placement of **{S}** relative to **{B}**. The optimization problem considered is the determination of the optimal location of the k points in a fixed anatomy manipulator's workspace so that the minimum value of the task based index will be maximum, ensuring that the best worst-case scenario for the manipulator will be determined.

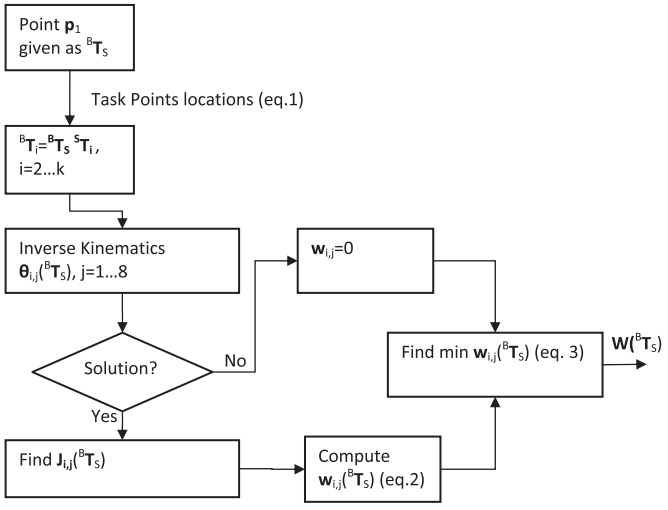

Fig. 4. Determination of the objective function.

Fig. 4 presents a flow chart of the procedure for determining the objective function for the considered problem.

For each point, the inverse kinematics problem of the manipulator is solved, providing a set of values for the joint variables required to reach the point. Since the task points are parametrically defined relative to **{S}**, which is located on the first point, the problem's variables are the location and the orientation of **{S}** relative to **{B}**.

At each point the value of the manipulability measure corresponding to each solution is calculated as

$$w_{i,j}(\boldsymbol{\theta}_{i,j}({}^{B}T_S)) = \sqrt{\det(\mathbf{J}(\boldsymbol{\theta}_{i,j}({}^{B}T_S))\cdot\mathbf{J}^T(\boldsymbol{\theta}_{i,j}({}^{B}T_S)))},$$
$$i=1,\ldots,k,\quad j=1,\ldots,8 \tag{2}$$

where i indicates the ith task point and j the corresponding solution to the inverse kinematics problem at the ith point (the maximum number of solutions obtained by analytically solving the inverse kinematics using the Product of Exponentials formula is 8 for 6 d.o.f. manipulators [12]), $\boldsymbol{\theta}_{i,j}$ is the vector of the joint angles, and $\mathbf{J}$ is the manipulator's Jacobean matrix.

The objective function for the determination of the optimal location of the points in the manipulator's workspace is the minimum of the manipulability index considering all points and is given by

$$W({}^{B}T_S) = \min_i(\min_j(w_{i,j}({}^{B}T_S)))\quad i=1,\ldots,k\quad j=1,\ldots,8 \tag{3}$$

where the optimization variables are considered to be the coordinates p_{1x}, p_{1y}, p_{1z} and the orientation $\mathbf{r}_1=[r_x,r_y,r_z]$ where r_x,r_y,r_z are the Euler angles defining **{S}** with respect to **{B}**. The objective function is to be maximized and the derived values of the optimization parameters allow the determination of the optimal location of all points in the manipulator's workspace.

4.2.2. Path following task

Common path following tasks performed by a robot in the manufacturing industry are painting, placing glue, arc welding, etc. The design of the process for such applications involves the placement of the trajectories inside the manipulator's workspace at a location where its performance is best, aiming at the increase of the end effector velocity and therefore reducing the required time to complete the task [1,2].

The problem considered is that the manipulator's end effector should follow m straight line segments, which are defined parametrically with respect to a local coordinate system **{S}** placed at the starting point of the first line segment whose position and orientation relative to **{B}** is given by the transformation $[{}^{B}\mathbf{T}_s]$.

Using a procedure similar to [1] it is possible to place this polyline at an optimal location inside the fixed anatomy manipulator's workspace. Given the location and orientation of the starting point frame **{$\mathbf{S_i}$}** and the ending point frame **{$\mathbf{F_i}$}** of each line segment and using a Taylor's algorithm [1], **{$\mathbf{S_n}$}** $n=1$, $N-2$ intermediate frames are determined along the segment. All frames, including the ending frame, are parametrically expressed with reference to frame **{S}**.

The index chosen in order to determine the optimal location of the path in the manipulator's workspace is the Manipulator Velocity Ratio (MVR) [1], given by

$$r_v = 1/\sqrt{\mathbf{u}_v^T(\mathbf{J}_v\mathbf{J}_v^T)^{-1}\mathbf{u}_v} \tag{4}$$

where $\mathbf{u}_v$ is a unit vector along the desired weighted end-effector velocity vector and $\mathbf{J}_v$ is the weighted Jacobean of the manipulator. The MVR depends not only on the robot configuration and the weighting matrices used, but also on the direction of the end effector velocity vector. The value of r_v provides a clear indication of the joint velocities required in order to move the end effector along a given direction with a desired velocity. As such, a high value of the MVR implies that the manipulator can move its end effector with the desired velocity along the required direction, utilizing minimum joint velocities. As with the point to point task presented in this work, a maxmin approach is used to determine the optimal location of the path in the manipulator's workspace, so that the minimum value of the MVR along the path would be maximum.

The global index along each segment, which is also the objective function is then given by

$$r_{vi}({}^{B}\mathbf{T}_S) = \min_n(r_{vn}({}^{B}\mathbf{T}_S), r_{vs}({}^{B}\mathbf{T}_S), r_{vf}({}^{B}\mathbf{T}_S)),$$
$$n=1,\ldots,N-2,\quad i=1\ldots m \tag{5}$$

where r_{vn}, r_{vs}, r_{vf} are the values of r_v at the nth intermediate frame, the starting frame and the ending frame of the ith path, respectively. The optimization variables are the location and orientation of the first frame of the first straight line segment **{S}** relative to **{B}** given by $[{}^{B}\mathbf{T}_s]$. Therefore the objective function considering all paths is given by

$$R_v({}^{B}\mathbf{T}_S) = \min_i(r_{vi}({}^{B}\mathbf{T}_S)),\quad \mathrm{i}=1\ldots\mathrm{m} \tag{6}$$

4.3. Optimal anatomy for a given task

The main advantage of the metamorphic robot is the adaptation of its anatomy to a given task, rather than locating the task in its workspace for a given anatomy. For the determination of the best anatomy the task points and the paths are considered fixed at the best location determined for the fixed anatomy counterpart of the metamorphic manipulator. The manipulator is now allowed to alter its anatomy, in order to determine that with the higher performance rating.

4.3.1. Point visiting task

For this particular stage, the optimization problem is defined as the determination of the optimal anatomy of the metamorphic manipulator maximizing the global minimum of the manipulability index as its end effector visits a number of points at a given location and orientation in its workspace.

The location of the points is considered fixed and the angles of the pseudo joints are required to be determined, in terms of the optimal manipulability performance. Therefore, the optimization variables are given by

$$\boldsymbol{\theta}_p = [\theta_a,\theta_b,\theta_c,\theta_d,\theta_e,\theta_f] \tag{7}$$

where $\boldsymbol{\theta}_p$ is the vector of the pseudo joint angles.

The manipulability index at each point for each joint value set resulting from solving the inverse kinematics problem is given by

$$w_{p_{i,j}}(\boldsymbol{\theta}_{i,j}(\boldsymbol{\theta}_p)) = \sqrt{\det(\mathbf{J}(\boldsymbol{\theta}_{i,j}(\boldsymbol{\theta}_p))\cdot\mathbf{J}^T(\boldsymbol{\theta}_{i,j}(\boldsymbol{\theta}_p)))},$$
$$i=1,\ldots,k,\quad j=1,\ldots,8 \tag{8}$$

where $\boldsymbol{\theta}_{i,j}$ is the vector of the six joint variables for the ith point, representing the jth solution to the inverse kinematics at that point.

The objective function considering all points is given by

$$W_p(\boldsymbol{\theta}_p) = \min_i(\min_j(w_{p_{i,j}}(\boldsymbol{\theta}_p)))\quad i=1,\ldots,k\quad j=1,\ldots,8 \tag{9}$$

The objective function should be maximized and the derived values of the optimization parameters $\boldsymbol{\theta}_p^*$ allow the determination of the best anatomy for the metamorphic manipulator:

$$\boldsymbol{\theta}_p^* = \arg(\max_{\boldsymbol{\theta}_p}(W_p(\boldsymbol{\theta}_p))) \tag{10}$$

4.3.2. Path following task

A similar procedure is followed for the determination of the best anatomy for a path following task. The straight line paths are fixed in the best location derived for the fixed anatomy manipulator. The optimization variables are once again the pseudo joint angles (Eq. (7))

Similarly to the process of determining the optimal location of the paths in the manipulator's workspace, a Taylor's algorithm is used to interpolate the end effector trajectory along each straight path. Therefore the global index for the MVR along each of the m segments is given by

$$r_{vpi}(\boldsymbol{\theta}_p) = \min_n(r_{vn}(\boldsymbol{\theta}_p), r_{vs}(\boldsymbol{\theta}_p), r_{vf}(\boldsymbol{\theta}_p)),$$
$$n = 1,\ldots,N-2, \quad i = 1\ldots m \tag{11}$$

Taking into account all the line segments, the best anatomy is determined by

$$\boldsymbol{\theta}_p^* = \arg(\max_{\boldsymbol{\theta}_p}(R_{vp}(\boldsymbol{\theta}_p))) \tag{12}$$

which is determined by maximizing the objective function:

$$R_{vp}(\boldsymbol{\theta}_p) = \min_i(r_{vpi}(\boldsymbol{\theta}_p)) \quad i = 1\ldots m \tag{13}$$

5. Application of the proposed approach for two case study tasks

Metamorphic manipulators are ideal for usage in SME's where small batches of different, customizable products are produced, according to customer specifications. Due to the custom nature of the produced products, usually different processes are required in their production, and therefore such tasks are mostly undertaken by human workers. The ability of metamorphic robots to allow the matching of their anatomy to a given task allows a single robot to undertake a wide variety of processes, while their rapid metamorphosis to the derived best anatomy for the task significantly reduces down times.

The following scenarios can be considered, for the application of metamorphic robots in different sectors of the manufacturing industry.

In steel construction industry, one of the standard assembly processes is the welding of smaller parts onto metal beams. The process involves spot welding of the smaller parts onto the beam so that it is steadily placed at the desired location and the consecutive welding of the part onto the beam along its edges in order to construct the final product. In the case of conducting this process using a metamorphic robot, the procedure can be separated into two parts. During the first part, the small metal parts are spot welded onto the metal beams at the desired locations. After this process is completed, the parts are then welded along one of their edges onto the beam in order to ensure the proper assembly. For each part of the process, the metamorphic manipulator's anatomy is set to that derived by the proposed method so as to present high performance.

In aircraft manufacturing, similar processes can be identified in subcontracting SME's. Usually these SME's undertake the production of fuselage or wing parts of small commercial or recreation aircraft for large manufacturers. Such processes involve firstly the precise positioning of the panels onto the skeleton and fastening to place either by riveting or spot welding and the subsequent drilling, countersinking, sealing and riveting of the panels in place [15]. In several cases, adhesives are used instead of the usual practice of riveting the panels in place [16]. The precise positioning of the panel into place can be considered as a point visiting task while the application of adhesive for panel bonding can be considered a path following task.

As seen, all of the above presented industrial processes involve both point to point and path following tasks. In the case of undertaking these processes by a metamorphic robot, the optimal anatomy for the point to point and path following parts of the desired process will have to be determined so as to ensure the best performance of the manipulator during the process.

Taking into account the possible application in aircraft manufacturing, a simplified process as the one described is considered. The construction of the wings of small commercial aircraft is to be undertaken by an SME. Small orthogonal panels are to be fitted onto the wing skeleton so as to form the wings. Such a process can be divided into two different processes. First the panels are to be spot welded onto the skeleton of the wing at their four corners for precise placement and fastening (point to point task). Secondly, after the riveting of all the panels onto the skeleton is performed, the panels are welded together along their edges (path following task). The optimal anatomies of the metamorphic manipulator are to be derived for each process using the proposed method.

In Fig. 5 a graphical representation of the considered tasks is illustrated. The first process is the riveting of the panel onto the wing skeleton by performing spot welding at its four corners (point visiting task). After this process is performed, the part is then welded along the edge between points $\mathbf{q_1}$ and $\mathbf{q_2}$ to its adjoining panel (path following task).

5.1. Point visiting task

In Fig. 5 the four task points for the riveting of the part are illustrated along with the local coordinate system of the first point **{S}**. For the sake of simplicity it is considered that the orientation with which the end effector approaches all points is identical to that of **{S}**. The transformation matrix, which presents the location and orientation of the **{S}** relative to **{B}** is given by

$${}^B\mathbf{T}_S = \begin{bmatrix} & {}^B\mathbf{R}_S & & q_{1x} \\ & & & q_{1y} \\ & & & q_{1z} \\ 0 & 0 & 0 & 1 \end{bmatrix} \tag{14}$$

where ${}^B\mathbf{R}_S$ is the 3×3 matrix representing the orientation of **{S}** relative to **{B}** and q_{1x}, q_{1y}, q_{1z} are the coordinates of **{S}** relative to **{B}**. The location and orientation of the coordinate systems of the other task points relative to **{S}** are

$${}^S\mathbf{T}_{S_2} = \begin{bmatrix} 1 & 0 & 0 & 0 \\ 0 & 1 & 0 & 0 \\ 0 & 0 & 1 & c \\ 0 & 0 & 0 & 1 \end{bmatrix}, \quad {}^S\mathbf{T}_{S_3} = \begin{bmatrix} 1 & 0 & 0 & 0 \\ 0 & 1 & 0 & b \\ 0 & 0 & 1 & c \\ 0 & 0 & 0 & 1 \end{bmatrix},$$

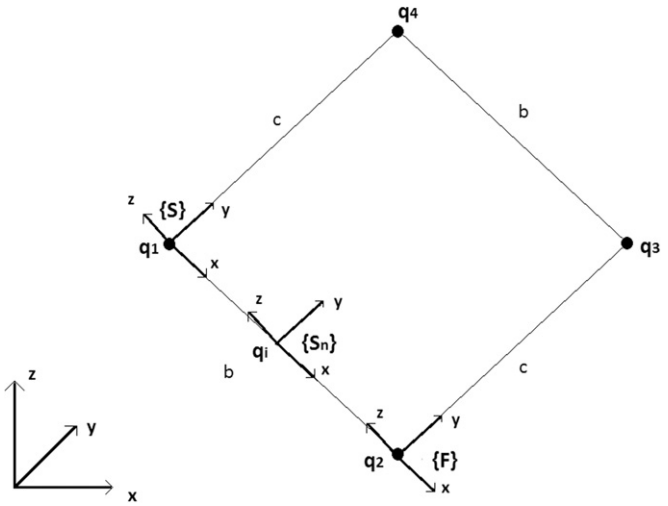

Fig. 5. The case study process considered.

$$ {}^{S}\mathbf{T}_{S_4} = \begin{bmatrix} 1 & 0 & 0 & 0 \\ 0 & 1 & 0 & b \\ 0 & 0 & 1 & 0 \\ 0 & 0 & 0 & 1 \end{bmatrix} \tag{15} $$

where $b=0.3$ m and $c=0.2$ m.

The process is located in the fixed anatomy manipulator's workspace by placing the task points at the best location determined by the maximization of the objective function given by Eq. (3). The optimization variables are considered to be the location and orientation of **{S}** relative to **{B}**.

A genetic algorithm was used in order to conduct the search of the optimum values for the optimization parameters, using the general procedure presented. The fitness function for the GA searching is the same as the objective function (Eq. (3)) and is given by

$$ fitness = W({}^{B}T_{S}) \tag{16} $$

For the determination of the optimal anatomy of the metamorphic system, the process is set at the derived location by the previous search and the manipulator is allowed to alter its anatomy via changing the pseudo joints angles until the anatomy with the best possible manipulability score is determined.

An exhaustive search algorithm was used in order to conduct the search for the optimal anatomy and the corresponding manipulability index is determined (Eq. (9)).

The algorithm determines the values of the elements of $\boldsymbol{\theta}_p^*$ (Eq. (10)) so as to maximize the objective function. Although the exhaustive search is time and resource demanding, it is used for this particular problem since it could provide an insight as to whether there could exist more than one anatomies of the metamorphic system that can present better performance than the fixed anatomy one. In order to simplify the procedure and limit the requirements in resources, the pseudo joint angles were limited to obtain values in the range of [0°,90°] except for θ_d where the range is [−90°,0°] at quantized intervals of 15°.

5.2. Path following task

Fig. 5 illustrates the local coordinate systems **{S}**,**{F}**, at the starting and ending frame of the edge to be welded and **{S_n}** of an intermediate point along the working edge. The local coordinate system **{S}** is such that its z axis is perpendicular to the surface of the part. The coordinate systems **{S_n}** and **{F}** are parametrically defined with respect to **{S}**. For the sake of simplicity, the orientation of the tool frame is considered to be fixed as it moves along the edge and identical to the determined orientation of the coordinate system of the starting point **{S}.**

The process is placed at the location inside the fixed anatomy manipulator's workspace determined by the maximization of the objective function given by Eq. (6). The optimization variables are position and orientation of **{S}** relative to **{B}**. The search was conducted using a GA in a similar fashion as with the point visiting task.

Then, the robot is allowed to alter its anatomy while the process remains fixed in the determined location so that the best anatomy for the task is determined. The global index was determined for each anatomy achieved by the metamorphic robot. The pseudo joint settings used are the same as those used for the point visiting task, and in a similar fashion an exhaustive search algorithm is used to conduct the search for the optimal anatomy.

6. Results and discussion

6.1. Point visiting task

A number of test runs are conducted in order to determine the best values for the GA parameters (probability of mutation, reproduction, etc.) for the task of placing the part in the fixed anatomy manipulator's workspace.

Since these parameters were determined, a significant number of runs were conducted using them, in order to determine the optimal values of the optimization variables as well as the corresponding best value of the objective function. Table 3 presents the results of four different runs, which are most representative of all. The resulting fitness function value for each placement of the points is presented in the first column, while the rest of the columns represent the value of each of the six joint angles of the fixed anatomy robot so as for it to reach **{S}** (Eq. (16)).

As seen in Table 3, the best value was achieved in run 4. The location and orientation of the tool frame for each of the points can be calculated using the robot's direct kinematics and Eqs. (14) and (15) (Table 4).

The location of the points in the manipulator's workspace, as determined by the GA's best run, is presented in Figs. 6 and 7. For the sake of simplicity only a portion (one quarter) of the whole workspace is presented.

For the second part of the search, the best anatomy of the metamorphic manipulator was sought for the given location of the process. The best results for the objective function as well as the corresponding anatomy in terms of the pseudo joint setting are presented in Table 5.

Table 3
Best results for the placement of the part in the fixed anatomy manipulator's workspace.

W	θ_1	θ_2	θ_3	θ_4	θ_5	θ_6
0.350831	259.07	85.09	88.02	210.25	190.58	180.15
0.344681	64.55	109.58	180.15	64.55	337.53	172.25
0.376994	142.83	334.24	56.02	339.50	166.014	62.67
0.411088	298.78	316.13	66.02	0	337.84	61.22

Table 4
Location of task points and orientation of tool frame relative to base coordinate system at each one as determined by the GA (lengths in meters).

Point	$\mathbf{g_{di}}$
$\mathbf{q_1}$	$g_{d1} = \begin{bmatrix} 1 & 0 & 0 & 2.2500 \\ 0 & 1 & 0 & -0.1500 \\ 0 & 0 & 1 & 2.1001 \\ 0 & 0 & 0 & 1 \end{bmatrix}$
$\mathbf{q_2}$	$g_{d2} = \begin{bmatrix} 1 & 0 & 0 & 2.2500 \\ 0 & 1 & 0 & -0.1500 \\ 0 & 0 & 1 & 2.3001 \\ 0 & 0 & 0 & 1 \end{bmatrix}$
$\mathbf{q_3}$	$g_{d3} = \begin{bmatrix} 1 & 0 & 0 & 2.2500 \\ 0 & 1 & 0 & 0.1500 \\ 0 & 0 & 1 & 2.3001 \\ 0 & 0 & 0 & 1 \end{bmatrix}$
$\mathbf{q_4}$	$g_{d4} = \begin{bmatrix} 1 & 0 & 0 & 2.2500 \\ 0 & 1 & 0 & 0.1500 \\ 0 & 0 & 1 & 2.1001 \\ 0 & 0 & 0 & 1 \end{bmatrix}$

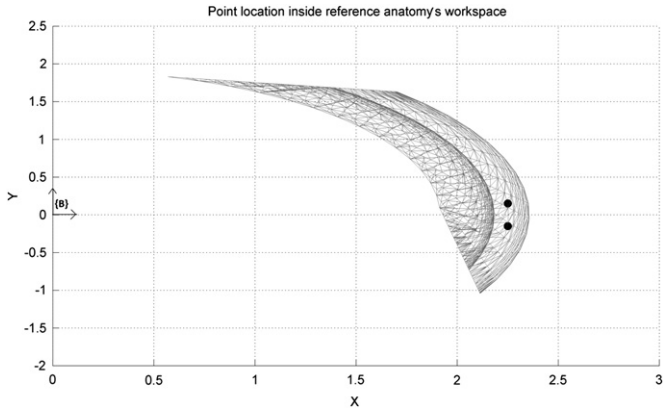

Fig. 6. Determined best location of task points in the fixed anatomy robot's workspace (x–y plane) (lengths in meters).

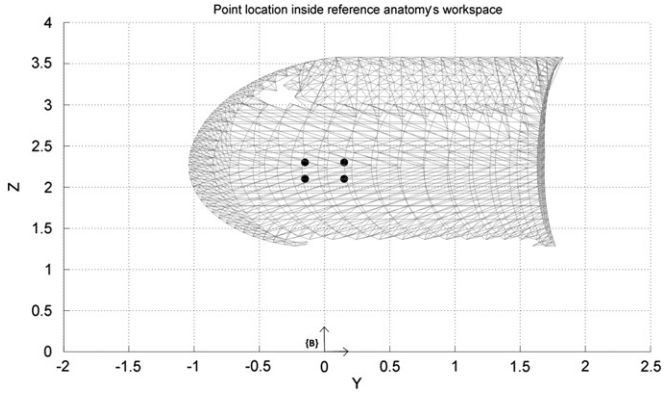

Fig. 7. Determined best location of task points in the fixed anatomy robot's workspace (y–z plane) (lengths in meters).

Table 5
Best anatomy for the metamorphic system.

W_p	θ_a	θ_b	θ_c	θ_d	θ_e	θ_f
2.1930	75	90	90	0	15	0

Using the equations depicted in Table 2, the twists of the active joints and the relative points on these twists required to determine the forward kinematics of the manipulator for this anatomy are depicted in Table 6, for the reference configuration of this anatomy ($\boldsymbol{\theta}=0$).

The corresponding anatomy at its reference configuration is depicted in Fig. 8.

Figs. 9 and 10 present the location of the task points in the best anatomy's workspace. For simplicity only a portion of the manipulator's workspace is presented.

Additionally, the following anatomies were also identified to present better performance than the fixed anatomy system (Table 7).

Comparing the best fitness function value achieved by the fixed anatomy system and the relative best value achieved by the metamorphic manipulator, it is clear that the latter manipulator can indeed present a far better performance than its fixed anatomy counterpart, even if the task was initially designed for the fixed anatomy robot. The overall increase in performance was at about 433%, which leaves little doubt about the increase in performance that can be achieved by the usage of metamorphic manipulators.

Table 6
Active joint twists and relative points for the best derived anatomy.

Joint	ω_i	p_i
1	$\begin{bmatrix}0\\0\\1\end{bmatrix}$	$\begin{bmatrix}0\\0\\0\end{bmatrix}$
2	$\begin{bmatrix}0.9659\\0\\0.2588\end{bmatrix}$	$\begin{bmatrix}0.9659L_2\\0\\L_1+0.2588L_2\end{bmatrix}$
3	$\begin{bmatrix}-0.2588\\0\\0.9659\end{bmatrix}$	$\begin{bmatrix}0.9659(L_4+L_3+L_2)\\0\\0.2588(L_4+L_3+L_2)+L_1\end{bmatrix}$
4	$\begin{bmatrix}0\\-1\\0\end{bmatrix}$	$\begin{bmatrix}0.9659(L_4+L_3+L_2)-0.2588L_5+0.8660(L_6+L_7)\\0\\L_1+0.2588(L_4+L_3+L_2)+0.9659L_5+0.5000(L_6+L_7)\end{bmatrix}$
5	$\begin{bmatrix}-0.5000\\0\\0.8660\end{bmatrix}$	$\begin{bmatrix}0.9659(L_4+L_3+L_2)-0.2588L_5+0.8660(L_6+L_7)\\0\\L_1+0.2588(L_4+L_3+L_2)+0.9659L_5+0.5000(L_6+L_7)\end{bmatrix}$
6	$\begin{bmatrix}0.8660\\0\\0.5000\end{bmatrix}$	$\begin{bmatrix}0.9659(L_4+L_3+L_2)-0.2588L_5+0.8660(L_6+L_7)\\0\\L_1+0.2588(L_4+L_3+L_2)+0.9659L_5+0.5000(L_6+L_7)\end{bmatrix}$

Using the forward kinematics of the fixed anatomy manipulator as they are constructed using the equations in Table 2, it is easy to define the manipulator's Jacobean determinant, which is the value of **w** as a function of the link lengths of the manipulator. Substituting the joint values as they are derived from the inverse kinematics problem for the point with the minimum **w** value yield the following equation:

$$w = 1.567L_4L_6L_7 + 0.783L_4(L_6^2+L_7{}^2) + 0.610L_4^2(L_6+L_7) \quad (17)$$

The relative equation of the best value of **w** for the best anatomy for the best configuration as a function of the manipulator lengths is

$$w_p = 0.455(L_2+L_3+L_4)(L_5L_7+L_5L_6) + 0.748(L_2+L_3+L_4)(L_7^2+L_6^2) + 1.496(L_2+L_3+L_4)L_7L_6 \quad (18)$$

Viewing the relation of the value of **w** for the two robots can provide some additional information on how the reconfigurable robot can achieve such a high increase in performance. As seen in Eqs. (17) and (18) the value of the index for the fixed anatomy robot is dependent on the product of three of the robots lengths, at the best configuration, as was expected, since the value of **w** is equal to the manipulability ellipsoid volume. However, the lengths from which its value depends on for the fixed anatomy robot have values that are smaller than one meter, and therefore their product is quite small. On the other hand, the reconfigurable robot's best anatomy is such that length L_3 is used for the determination of the value of the manipulability index, which is the only length of the robot that is more than one meter in value. Comparing the dominant terms of both equations (using the length values provided for the case study robot), these present values $1.567L_4L_6L_7 = 0.1567$ for the fixed anatomy system and $1.496(L_2+L_3+L_4)L_7L_6 = 0.8602$. This significant increase is the main reason for the much higher value of the performance index achieved by the reconfigurable robot's best anatomy.

Table 8 presents the manipulator link twists (D–H representation) for the determined best anatomy. These are computed by determining the orientation and location of the active joint twists using the equations provided in Table 2, and determining their relative orientation in pairs, so as to measure their angle.

As seen, in comparison to the fixed anatomy system, the best anatomy is completely different than that of the fixed anatomy system, since the first link twist is now 75° and the second has become 90°. Moreover, the derived anatomy is not "in line" with

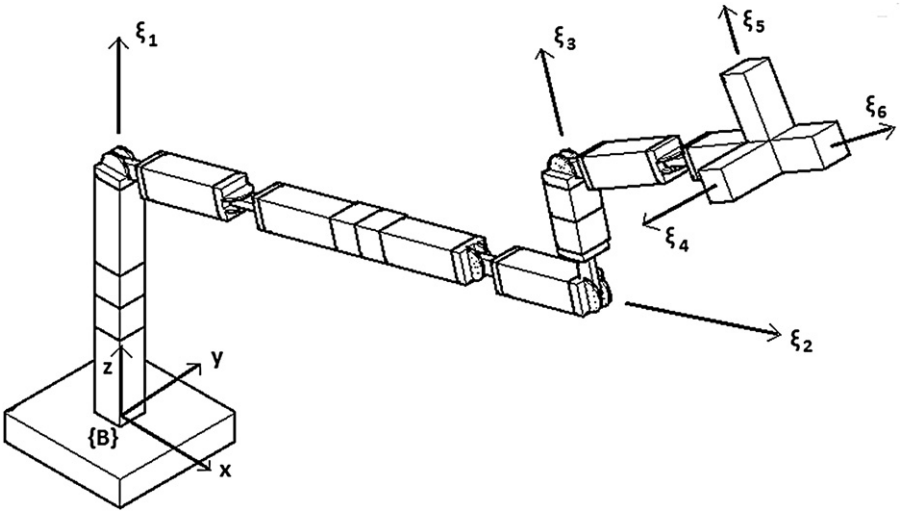

Fig. 8. Best anatomy determined for the point visiting task.

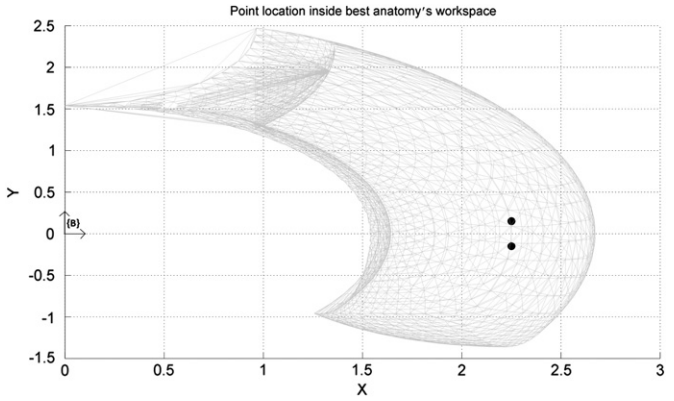

Fig. 9. Task points locations in the best anatomy's workspace (x–y plane) (lengths in meters).

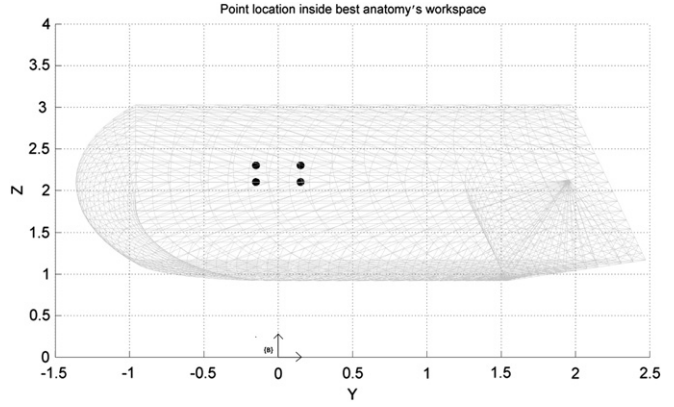

Fig. 10. Task points locations in the best anatomy's workspace (y–z plane) (lengths in meters).

current design practice, since the first link twists are different than 0° or 90°. Additionally, as seen in Table 9 all the best derived anatomies also present the same anatomical configuration and are not "in line" with current design practice. This is an indication that such anatomies could present better performance than those currently in use.

Fig. 11 presents a bar chart categorizing the number of anatomies achieved by the metamorphic system according to the fitness function value they achieved. As seen, the vast

Table 7
Additional anatomies with better performance than the fixed anatomy robot.

W	θ_a	θ_b	θ_c	θ_d	θ_e	θ_f
2.1927	75	90	0	−90	30	0
2.1405	75	90	90	0	30	0
2.1320	75	75	90	0	15	0
2.1235	75	75	90	0	15	15
2.0479	75	90	90	0	15	15
2.0365	75	90	90	0	30	15
2.0277	75	60	90	0	15	0

Table 8
Link twists of the robot at the derived best anatomy.

Joint pair	ξ_1 and ξ_2	ξ_2 and ξ_3	ξ_3 and ξ_4
Link twist angle (deg.)	75	90	90

Table 9
Best GA runs for the fixed anatomy manipulator.

R_V	θ_1	θ_2	θ_3	θ_4	θ_5	θ_6
0.769798	57.13	35.21	281.72	49.77	251.90	230.63
0.660986	31.99	43.28	313.77	233.41	62.60	210.30
0.749805	326.15	208.37	313.77	233.41	62.60	210.30

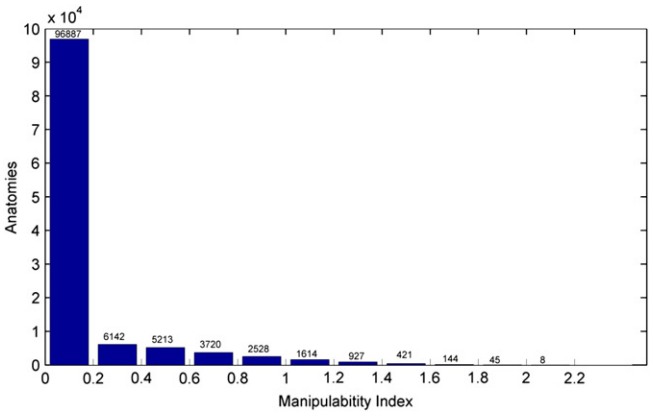

Fig. 11. Anatomies number depending on the fitness function value achieved.

majority of them lie around the optimal value of the objective function achieved by the reference fixed anatomy system. However, a significant number of anatomies can achieve a better performance than the fixed anatomy system, with 8 of them presenting a staggering increase in performance.

The presented results, regarding the point visiting task strongly indicate the fact that the determination of the best anatomy for a given task can achieve better results in performance as opposed to the determination of the best location of the task in a specific anatomy's workspace. Therefore the practical advantages of replacing a fixed anatomy robot with a metamorphic one in a robotic workcell will not only increase its capacity to perform different tasks, but through the matching of different anatomies to different tasks will also cause a sharp increase in overall performance.

6.2. Path following task

Using the method presented the line segment was first placed in the fixed anatomy robot's workspace so that the manipulator presents the best velocity performance. The maximum allowed error for the Taylor's interpolation was 10^{-4} m. The best runs of the GA yielded the following results for the global MVR index and location of the starting point of the line segment (Table 9). The resulting fitness function value for each placement of the points is presented in the first column, while the rest of the columns represent the value of each of the six joint angles of the fixed anatomy robot so as for it to reach **{S}**.

Table 10
Best anatomies and relative global index value for the metamorphic system.

R_{Vp}	θ_a	θ_b	θ_c	θ_d	θ_e	θ_f
1.2516	15	0	15	−90	45	60
1.2309	0	0	0	−75	45	60
1.2174	0	0	15	−90	30	45
1.2147	15	0	15	−90	60	75
1.2055	15	0	0	−75	45	45
1.2046	15	0	0	−75	45	60

As seen, the best run was the first one where the global index value achieved was 0.769798.

Using the now placed segment, the manipulator is allowed to alter its anatomy in order to address the task. The ten best anatomies and the relative value of the global MVR index are presented in Table 10.

As seen in Table 10, the metamorphic manipulator is once again able to increase its performance for a given task, as opposed to a fixed anatomy robot. The significantly increased global MVR index value signifies that the new anatomy derived for the metamorphic robot can move its end effector along the task line segment with the same velocity as the fixed anatomy one however requiring limited joint velocities. This implies that since this method presents the best worst case scenario for the task execution the metamorphic robot is indeed capable of achieving greater performance for the given task.

Fig. 12 illustrates the anatomy that achieved the best global MVR index.

Comparing the best anatomies derived for the two tasks (Figs. 8 and 12) it can be seen that the metamorphic robot altered its anatomy so that for the point visiting task it would achieve a greater reach in the x–y direction therefore placing the points in a location in its workspace that it would present the best manipulability performance, while for the path following task, the new anatomy was such that the movement of the end effector along the path direction would approach in a better way the directions of motion in which the MVR values are high.

Fig. 13 illustrates the MVR value achieved by the best anatomy of the metamorphic robot at the points derived along the path by the Taylor's algorithm.

As seen in Fig. 13, the index value at the derived intermediate points visited along the path is much higher that the global MVR value achieved by the fixed anatomy robot. This is a clear indication of the increase in performance achieved via the changing of the manipulator's anatomy.

Table 11 presents the link twists (D–H representation) as computed using Table 2.

As seen in Table 11 the best anatomy derived for the task is completely different than the reference anatomy, since the second

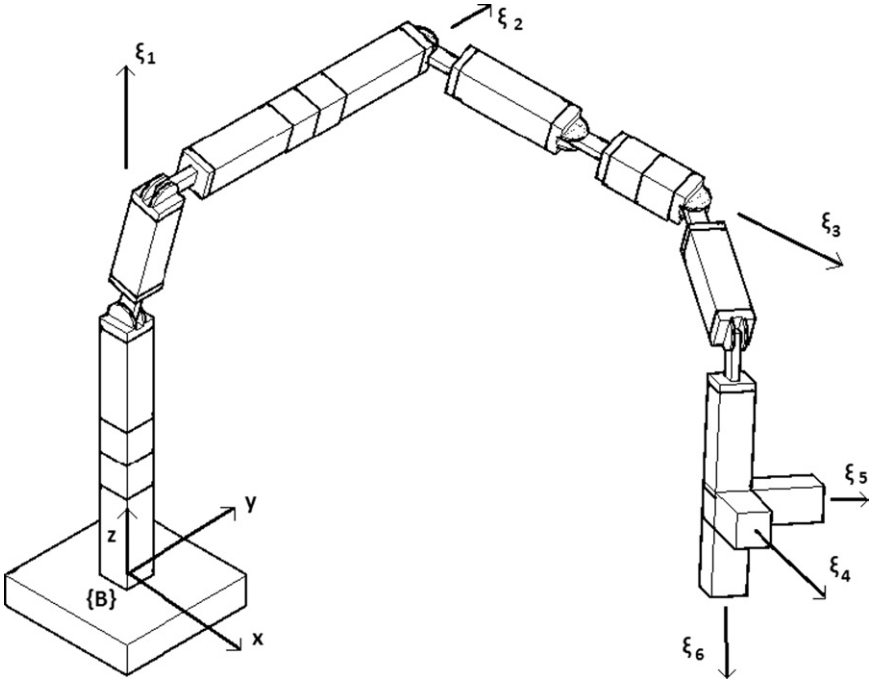

Fig. 12. Best anatomy for the path following task.

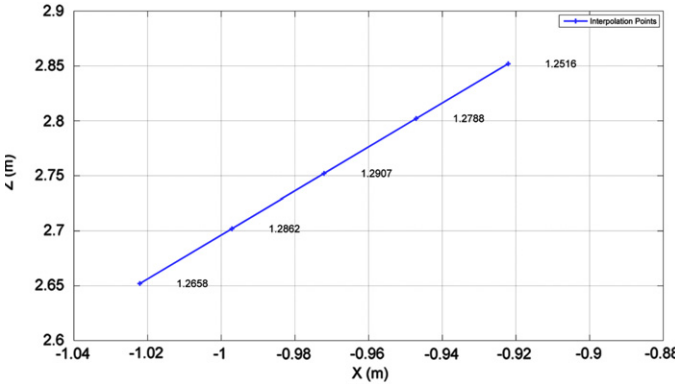

Fig. 13. MVR index value at the interpolation points along the path (lengths in meters).

Table 11
Link twists of the robot at the derived best anatomy.

Joint pair	ξ_1 and ξ_2	ξ_2 and ξ_3	ξ_3 and ξ_4
Link twist angle (deg.)	90	75	45

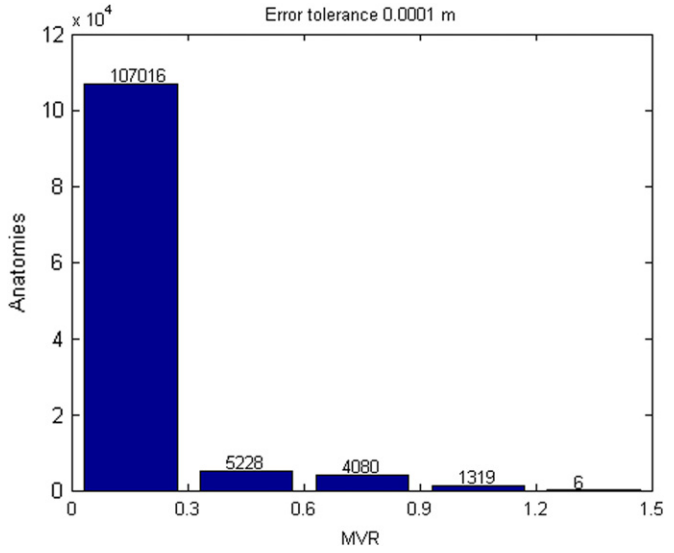

Fig. 14. Grouping of anatomies with respect to global MVR index value.

and third link twists have changed. The derived best anatomy is different from current design practice since it presents two link twists different than the usual 0° or 90°, another indication that such anatomies could present a better performance than those currently in usage.

Fig. 14 presents a grouping of the possible anatomies achieved by the metamorphic manipulator with respect to the global index value achieved.

As with the case of the manipulability index for the point to point path, it is made clear that the metamorphic system can present a wide range of anatomies achieving higher performance than the fixed anatomy system for the path following task presented.

7. Conclusions

An approach for the determination of the best anatomy for a class of metamorphic serial link manipulators for two types of common industrial robotic tasks is presented. First a point to point visiting task is considered to be fixed at a location inside the robotic workcell's area, where a fixed anatomy manipulator would present the best performance in terms of manipulability. Then a path following task is considered to be fixed where a fixed anatomy manipulator would present the best performance in terms of velocity performance. The fixed anatomy robot is then replaced by the metamorphic one and the best anatomy in terms of the selected performance measure is determined for both tasks based on the proposed approach. The presented method is then utilized for a simplified application of an assembly task in aircraft production, where a The outer shell of a wing is assembled by placing smaller metal plates onto the wing skeleton. First the part is spot welded onto the skeleton and then it is welded to the neighboring part along one of its edges.

The results show two main conclusions. Firstly the presented method allows the matching of the best anatomy of the metamorphic robot to a task in order to increase its kinematic performance during task execution. Secondly, since the tasks were fixed in the workspace of a fixed anatomy robot, a comparison of the results is made capable, which strongly hints that metamorphic robots could indeed show far better performance, than fixed anatomy manipulators. Furthermore, it is possible to enhance the metamorphic robot's performance even further by conducting a search not only for the best anatomy for a task but also for the best placement of the task for each anatomy.

Future work will include a method for conducting a search for the best anatomy and task placement simultaneously. Additionally, the usage of A.I. methods such as genetic algorithms and ANFIS systems will decrease the required high computational time of such a method. Finally, the construction of the presented concept for passive connecting modules presented (pseudo joints) for constructing the proposed class of metamorphic manipulators will allow further experimentation with real life models of manipulators and further augmentation of the presented method, such as including different performance indices and other types of tasks.

References

[1] Nektarios A, Aspragathos N. Optimizing velocity performance of a position and orientation path following task. Robotics and Computer Integrated Manufacturing 2010;26(2):162–73.
[2] Aspragathos N, Foussias S. Optimal location of a robot path when considering velocity performance. Robotica 2002;20:139–47.
[3] Feng X, Holmgren B, Olvander J. Evaluation and optimization of industrial robot families using different kinematic measures. In: Proceedings of the 2009 ASME international design engineering technical conferences and computers and information in engineering conference, DETC2009, San Diego, CA; 30 August–2 September 2009.
[4] Mayorga R, Carrera J, Oritz M. A kinematics performance index based on the rate of change of a standard isotropy condition for robot design optimization. Robotics and Autonomous Systems 2005;53:153–63.
[5] Kucuk S, Bingul Z. Robot workspace optimization based on a novel local and global performance indices. In: Proceedings of the IEEE international symposium on industrial electronics, Dubrovnik, Croatia; June 20–23, 2005. p. 1593–98.
[6] Chen I-M. Rapid response manufacturing through a rapidly reconfigurable robotic workcell. Robotics and Computer Integrated Manufacturing 2001;17:199–213.
[7] Yang G, Chen I-M. Task-based optimization of modular robot configurations: minimized degree of freedom approach. Mechanism and Machine Theory 2000;35:517–40.
[8] Lemay J, Notash L. Configuration engine for architecture planning of modular parallel robots. Mechanism and Machine Theory 2004;39:101–17.
[9] Paredis C, Brown B, Khosla P. A rapidly deployable manipulator system. In: Proceedings of the international conference on robotics and automation; 1996. p. 1434–39.
[10] Schonlau W. RMMS: A modular robotic system and model based control architecture. Proceedings of SPIE—The International Society for Optical Engineering 1999;3839:289–96.

[11] Hafez M, Lichter M, Dubowsky S. Optimized binary modular reconfigurable robotic devices. IEEE/ASME Transactions on Mechatronics 2003;8(1):18–25.
[12] Valsamos H, Aspragathos N. Determination of anatomy and configuration of a reconfigurable manipulator for the optimal manipulability. In: Proceedings of the ASME/IFToMM international conference on reconfigurable mechanisms and robots, London; 2009. p. 497–503.
[13] Valsamos H, Moulianitis V, Aspragathos N. A generalized method for solving the kinematics of 3 d.o.f. reconfigurable manipulators. In: Proceedings of the I*PROMS 2009 virtual conference; 2009.
[14] Gao Y. Decomposible closed-form inverse kinematics for reconfigurable robots using product of exponential formula. Master Thesis. School of Mechanical and Production Engineering Nanyang Technological University; 2000.
[15] Jayaweera N, Webb P. Adaptive robotic assembly of compliant aero-structure components. Robotics and Computer-Integrated Manufacturing 2007;23(2): 180–94.
[16] Higgins A. Adhesive bonding of aircraft structures. International Journal of Adhesion and Adhesives 2000;20(5):367–76.